The Electrochemistry of a Gelatin Modified Gold Electrode

Karolien De Wael[1,†], Annelies Verstraete[1], Sandra Van Vlierberghe[2], Winnie Dejonghe[3],
Peter Dubruel[2], Annemie Adriaens[1,]*

[1] Department of Analytical Chemistry, Ghent University, Krijgslaan 281 S12, B-9000 Ghent, Belgium
[2] Polymer Chemistry and Biomaterials Research Group, Ghent University, Krijgslaan 281 S4bis, B-9000 Ghent, Belgium
[3] Separation and Conversion Technology, Flemish Institute for Technological Research (VITO), Boeretang 200, B-2400 Mol, Belgium
[†]New address as of April 2011: Chemistry Department, University of Antwerp, Universiteitsplein 1, B-2610 Antwerp, email: karolien.dewael@ua.ac.be
The authors wish it to be known that, in their opinion, the first two authors should be regarded as joint first authors.
[*]E-mail: annemie.adriaens@UGent.be

This paper discusses the electrochemical behaviour of gelatin coated gold electrodes in physiological pH conditions in a potential window −1.5 till 1.0 V vs SCE by performing cyclic voltammetry. A comparison is made between gelatin A and gelatin B, which have respectively a positive and a negative net charge at physiological pH. The deposition of gelatin onto the gold surface is confirmed by means of attenuated total reflection-infrared (ATR-IR) spectroscopic analyses.

1. INTRODUCTION

Gelatin is a widely applied agent due to the fact that it is natural, nontoxic, biodegradable, biocompatible in physiological environments, edible and water permeable [1]. This inexpensive macromolecule is used as a gelling, thickening, binding, film forming and stabilizing agent in different industries including food, pharmaceutical and cosmetic industry. Gelatin also finds applications in photography and some specialized industries [2].

Gelatin is a water soluble protein possessing a high average molecular weight (distribution range: 15-250 kDa [3]) consisting of various amino acids, with glycine, proline and hydroxyproline being the most abundant [4]. It is derived from collagen, the major structural protein in the connective tissue of animal skin and bones. Because of their different origin and manufacturing process, one can distinguish different types of gelatin, with type A and type B gelatin being the most common [5]. Type A gelatin results from acidic hydrolysis of collagen and features an iso-electric point (IEP) of 6.0-8.0. Type B gelatin is obtained from an alkaline treatment of collagen which causes a greater degree of deamidation of asparagine and glutamine converting these amino acids into aspartic acid and glutamic acid, respectively [6]. The larger number of free carboxyl groups results in a lower IEP of type B gelatin (4.7-5.3).

Because of the physical interactions between the protein chains (e.g. van der Waals forces and hydrogen bonds between amino acids) gelatin is an example of a physically cross-linked hydrogel. Hydrogels are hydrophilic polymer networks which swell considerably in an aqueous medium by absorbing water without dissolving [7]. The hydrophilic groups or domains which are hydrated make gelatin a suitable matrix for the entrapment of several biomolecules because of its excellent biocompatibility. The incorporated biomolecules are hydrated and can maintain their native configuration. Enzymes that have been incorporated so far in a gelatin matrix, in order to construct an electrochemical biosensor, include amongst others glucose oxidase [8,9], α-glucosidase [10], acetylcholinesterase [11]. In addition, configurations embedding more than one enzyme in gelatin have already been developed [12,13].

Although different research groups have reported on the use of gelatin as immobilization matrix, the electrochemical behaviour of gelatin studied at electrode surfaces has not been published yet to the best of our knowledge. In this paper we discuss the electrochemistry of a gelatin modified gold electrode. In addition, attenuated total reflection-infrared (ATR-IR) spectroscopic analyses were performed to confirm the deposition of gelatin on the electrode surface. A fundamental, electrochemical study of gelatin at a gold electrode, as presented in this work, is of great value for further research in which enzymes are incorporated in a gelatin matrix.

2. MATERIAL AND METHODS

2.1. Chemicals and solutions

Sodium hydroxide and 2-[4-(2-hydroxyethyl)-piperazinyl]ethanesulfonic acid (HEPES) were purchased from Sigma-Aldrich. The HEPES buffer solution of 10 mmol.L^{-1} was set to pH 7.0 using a 0.15 mol.L^{-1} NaOH solution. Type B gelatin (IEP = 5, Bloom strength = 257), isolated from bovine skin by the alkaline process, was kindly supplied by SKW Biosystems (Ghent, Belgium). Type A gelatin (IEP = 8.8, Bloom strength = 202), isolated from porcine skin by the acid treatment, was obtained from Rousselot (Ghent, Belgium).

2.2. Electrode preparation

Inlaid gold working electrodes of 1.6 mm diameter (BASi, UK) were pre-treated by mechanical polishing. Prior to its first use, the electrode surface was scoured briefly on SiC-emery paper 1200 grit to obtain an active surface. To smoothen this relatively rough surface, it was further subjected to sequential polishing using a cloth covered with alumina powder (Buehler, Illinois, USA) of 1 and 0.05 µm particle size, both during 10 min. To remove any adherent Al_2O_3 particles, the electrode surface was rinsed thoroughly with deionised water and cleaned in an ultrasonic bath (Branson 3210) for 5 min.

The deposition of gelatin onto a gold electrode was performed as follows: a gelatin solution was prepared by stirring the gelatin A or B powder (0.5 g) and the HEPES buffer solution (10 mL) at 40 °C. A total of 5 µL of this gelatin solution (5 w/v%) was brought onto the electrode surface using a syringe. These electrodes are in the text referred to as GelA|Au or GelB|Au depending on whether gelatin A or gelatin B is used. All the electrodes were exposed to air for 2 h at 4 °C. Finally, the electrodes were washed with the HEPES buffer solution before further experiments.

2.3. Apparatus

Experiments were run in parallel by using two potentiostats to record voltammetric curves: a PGSTAT20 and a PGSTAT302N potentiostat, controlled by GPES 4.9 005 and NOVA 1.5 software package, respectively (both ECO Chemie, the Netherlands). The basic electrochemical set-up consisted of a three-electrode cell using a saturated calomel reference electrode (SCE, E = 0.241 V vs SHE at 298 K, Radiometer Analytical, France) and a platinum counter electrode. The electrochemical cell is filled with the pH 7.0 HEPES buffer solution (10 mmol.L^{-1}, unless stated otherwise). Prior to the start of each measurement, the pH of the buffer cell solution was measured using an Orion Benchtop pH-meter model 420A (Thermo Fisher Scientific, USA). The cell solution was thoroughly deoxygenated by bubbling nitrogen through it for 20 min prior to the measurements and a nitrogen atmosphere was maintained over the solution during the experiment.

Attenuated total reflection-infrared (ATR-IR) spectroscopic analyses were performed in order to obtain qualitative proof of the deposition of gelatin onto the gold electrode. ATR-IR spectra were acquired using a Biorad FT-IR spectrometer FTS 575C equipped with a 'Golden Gate' ATR accessory. The latter was fitted with a diamond crystal. The coating covering the electrode surface was measured directly by pressing the electrode against the ATR crystal. The spectra were recorded over the range 4000-600 cm^{-1} and averaged over 16 scans.

3. RESULTS AND DISCUSSION

Gelatin modified gold electrodes were prepared by the method described in the experimental part. Gelatin B was selected first and after being immobilized onto a gold electrode, the modified surface was characterized spectroscopically (part 1) and electrochemically (part 2). Finally, a comparison was made with the electrochemical behaviour of gelatin A deposited on a gold electrode.

3.1. ATR-IR characterization of a gelatin modified gold electrode

Figure 1 shows the ATR-IR spectra of a bare gold electrode (1) and a GelB|Au electrode (2). The observed IR spectrum of the latter is in agreement with previous reported results [14,15]. The most characteristic regions of protein IR spectra include the amide A and B, the amide I, II and III bands [16]. The N-H stretching vibrations in gelatin give rise to the amide A band at 3304 cm^{-1} and the weaker amide B band at 3080 cm^{-1}. The amide I band at 1630 cm^{-1}, which is the most intense absorption band in proteins, primarily represents the carbonyl C=O stretching vibrations of the polypeptide backbone. The amide II band at 1539 cm^{-1} is mainly due to the coupling of the bending of the N-H bond and the stretching of the C-N bond. Several peaks are present in the 1400-1200 cm^{-1} region, which is known as the amide III mode. The composition of this region is more complex, since N-H bending contributes to several peaks in this region [16]. In addition to the above-mentioned amide bands, also other absorption bands in the spectrum can be attributed. The peaks in the 2800-3000 cm^{-1} region correspond to C-H stretching vibrations. The C-H bending vibrations are responsible for the band at 1450 cm^{-1}. The C-O stretch induces the 1082 cm^{-1} band and the peak at 1034 cm^{-1} can be explained by skeletal stretches [17,18]. Overall, the results clearly demonstrate the presence and therefore the deposition of gelatin onto gold.
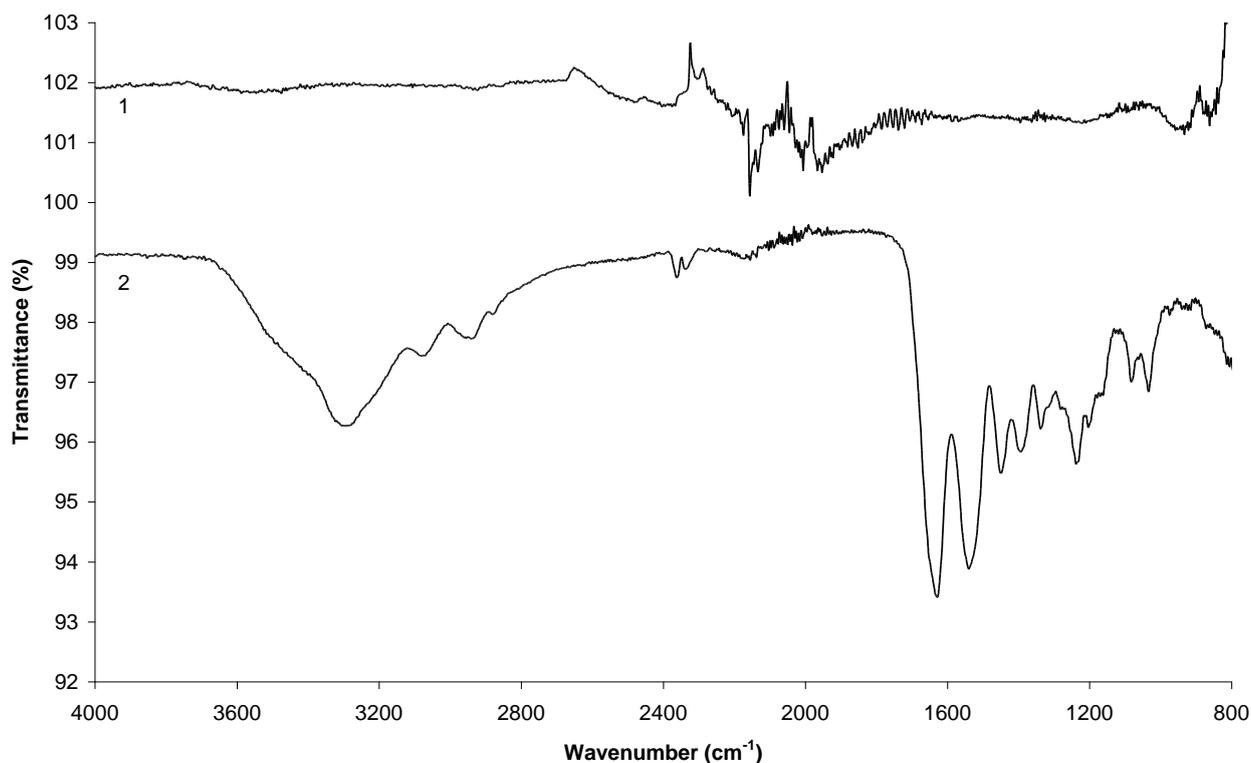

Figure 1. ATR-IR spectra of Au (1) and GelB|Au (2) electrodes.

3.2. Electrochemical characterization of GelB immobilized on a gold electrode

Figure 2 shows the electrochemical response of a bare gold electrode (dashed line) and a GelB|Au electrode (full line) in a 10 mmol.L^{-1} HEPES pH 7 buffer solution in a potential window from −1.5 till 1.0 V with a scan rate of 50 mV.s^{-1}. The voltammogram of the bare gold electrode shows an oxidation wave I_a at 0.9 V and a reduction process I_c at 0.6 V which can be attributed to the oxidation of the gold surface and reduction of the gold oxide formed during this surface oxidation [19]. Two other redox processes are observed at 0.45 V (II_a) and −1.1 V (II_c). The voltammetric scan of GelB|Au shows that the peak attributed to gold oxide formation (I_a) and its reduction (I_c) have decreased remarkably. Another reduction peak is observed at 0.35 V (III_c). In what follows, the nature of the processes II_a, II_c and III_c will be studied in more detail.
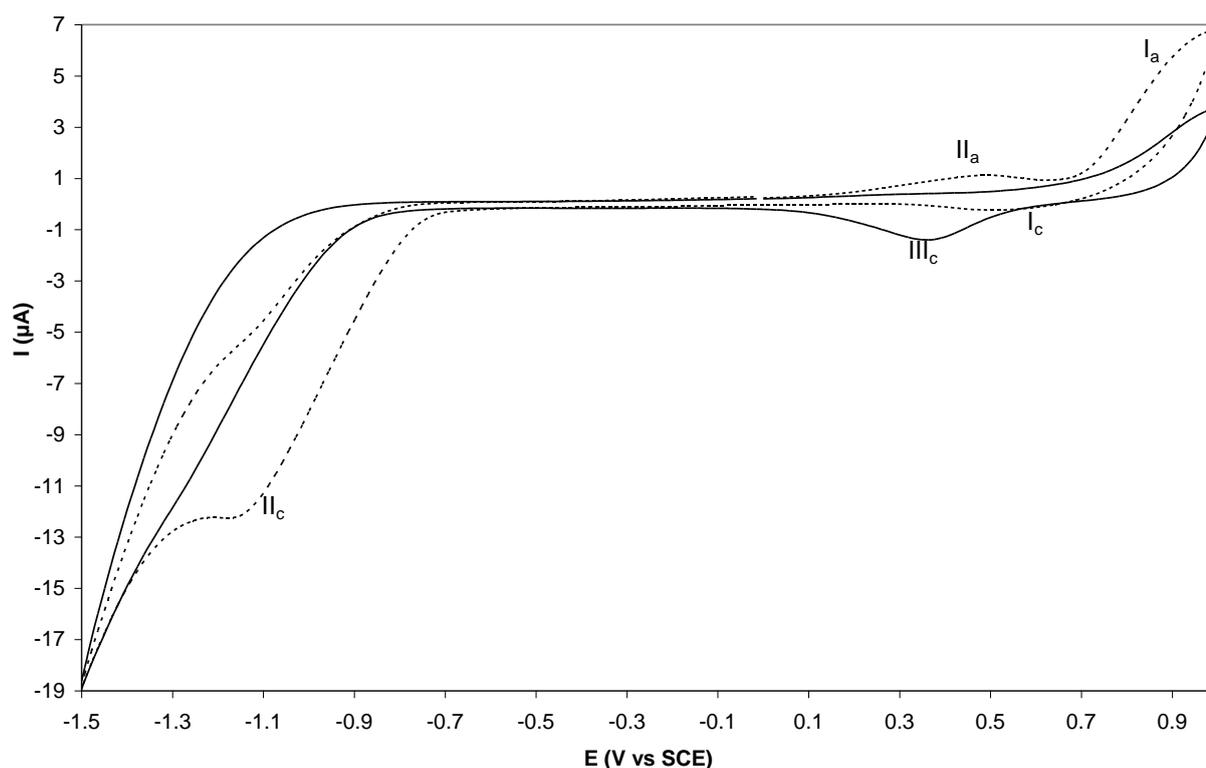

Figure 2. The current potential behaviour of a bare gold electrode (dashed line) and a GelB|Au electrode (full line) in a 10 mmol.L^{-1} HEPES pH 7 buffer solution with a scan rate of 50 mV.s^{-1} in a potential window from −1.5 till 1 V.

To reveal the nature of processes II_a and II_c, the concentration of the HEPES buffer solution was varied. The prepared concentrations were 10, 25, 50, 75 and 100 mmol.L^{-1}. Figure 3 represents the first cyclic voltammogram recorded at a GelB|Au electrode in three of the mentioned HEPES solutions: 10 (1), 50 (2) and 100 mmol.L^{-1} (3). A linearly dependence of the HEPES concentration is observed for the cathodic current II_c, which is confirmed by the calibration curve, obtained by plotting the peak current at ca. −1.45 V as a function of the HEPES concentration (inset Figure 3).

To prove the relationship between the redox reactions II_a and II_c, the potential window was adjusted to -0.6 till 1.0 V (scan 20, Figure 4). By changing the negative limit of the potential window, the reduction process II_c does no longer take place. As a consequence, the oxidation reaction II_a is much less pronounced, as can be derived from the 20th cyclic voltammetric scan shown in Figure 4. Based on the above described experiment, the redox processes II_a and II_c can be explained as a coupled redox reaction in which HEPES is involved.
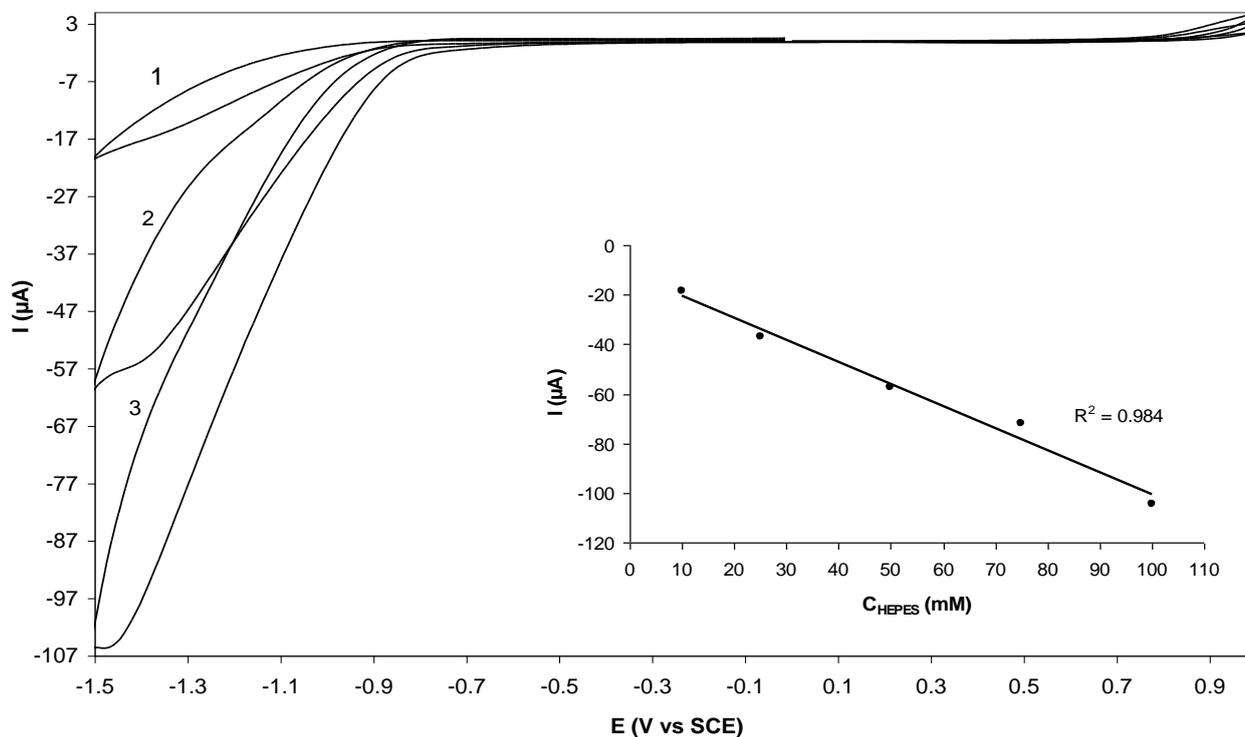

Figure 3. The current potential behaviour of a GelB|Au electrode in a HEPES pH 7 buffer solution with different HEPES concentration: 10 (1), 50 (2) and 100 (3) mmol.L^{-1}. Inset: calibration curve.

In the next paragraph, we focus on the reduction process III_c at ca. 0.4 V. Based on the comparison between the electrochemical behaviour of a bare gold electrode and a GelB|Au electrode (Figure 2), it is clear that gelatin is involved in this process as this reduction peak is absent in the case of a bare gold electrode. However, the rather asymmetric shape of this peak suggests there is also another reduction process which occurs at this potential, resulting in the superposition of two processes. To clarify this, voltammetric curves of a bare gold electrode and a GelB|Au electrode were recorded in the potential window -0.6 till 2.0 V.

Figure 5 represents scan 3 of the obtained cyclic voltammogram recorded at the Au electrode (dashed line) and scan 3 (1) and scan 20 (2) in the case of the GelB|Au electrode (full lines). Figure 5 shows that the reduction peak III_c shifts towards a more positive potential as a function of the number of scans, i.e. it shifts towards the reduction of gold oxide (I_c). This phenomenon can be explained by

the roughening of the gold surface by oxidation and reduction of the formed gold oxides which is described in literature [20]. The formation of higher gold oxides at the GelB|Au electrode was confirmed visually: the initially bright gold surface has become red brown after potential cycling [21].
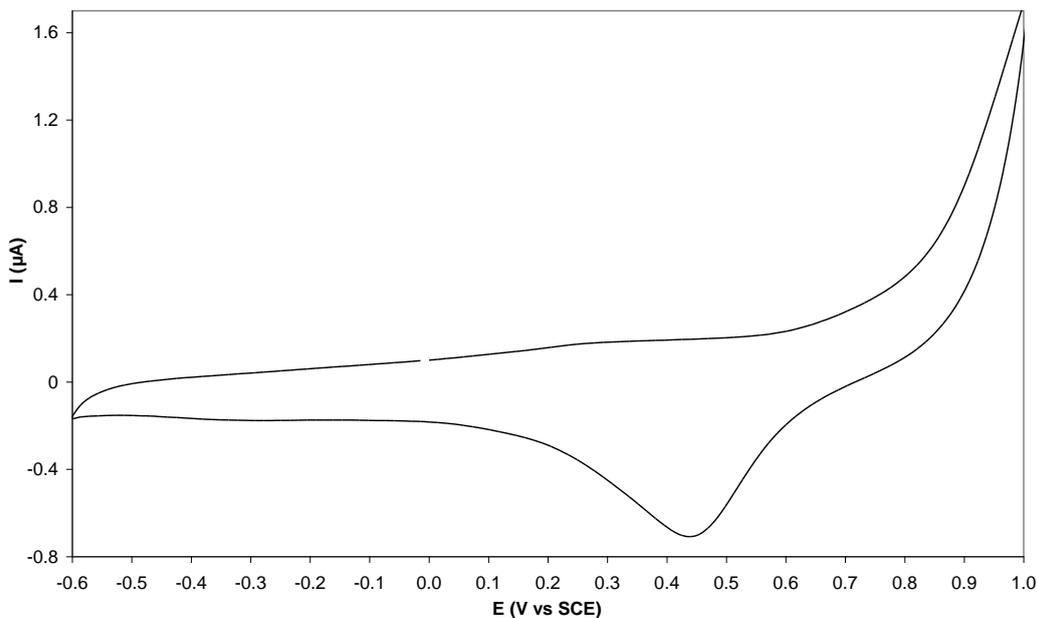

Figure 4. The current potential behaviour of a GelB|Au electrode in a 10 mmol.L^{-1} HEPES pH 7 buffer solution with a scan rate of 50 mV.s^{-1} in a potential window from -0.6 till 1 V: scan 20.
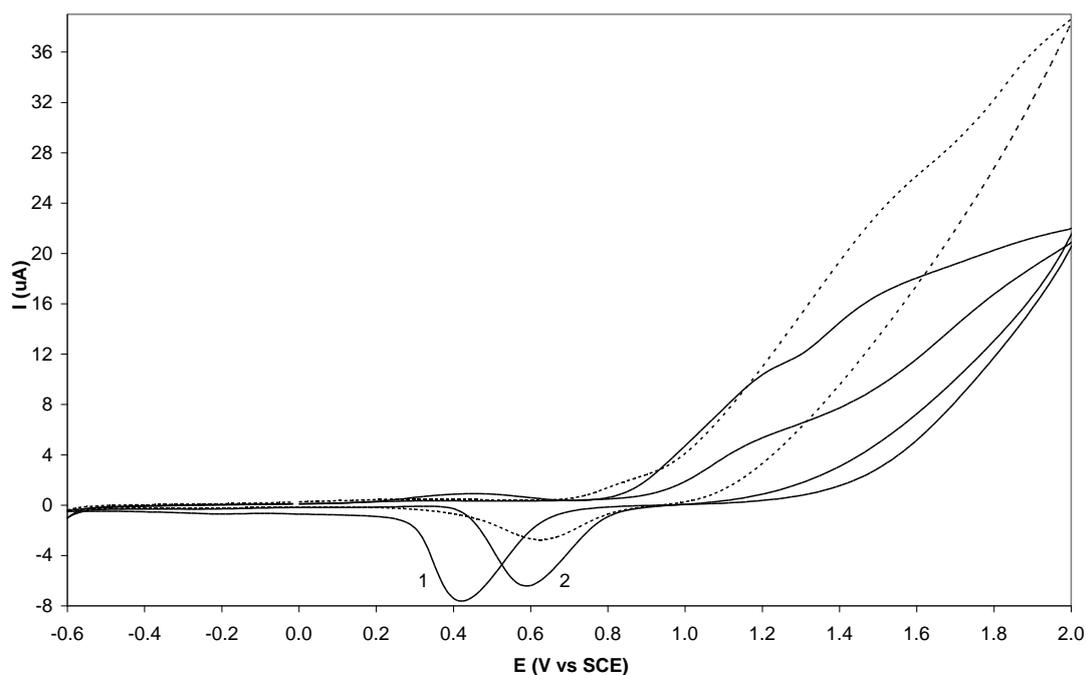

Figure 5. The current potential behaviour of a bare gold electrode (dashed line, scan 3) and a GelB|Au electrode (full line) in a 10 mmol.L^{-1} HEPES pH 7 buffer solution with a scan rate of 50 mV.s^{-1} in a potential window from -0.6 till 2 V as a function of scan number: scan 3 (1) and 20 (2).

According to the authors, during cycling the roughening results in damaging the gelatin layer, which makes the gold surface more accessible and as a consequence the reduction I_c is more pronounced. Based on these observations, we conclude the reduction process III_c to be composed of a reduction process in which gelatin is involved on the one hand and the reduction of gold oxide on the other hand. The latter process is enhanced when enlarging the potential window to 2.0 V as the oxidation of gold is more pronounced at this extreme positive potential.

Figure 6 shows a selected number of the 20 cyclic voltammetric scans recorded at a GelB|Au electrode in a 10 mmol.L^{-1} HEPES pH 7 buffer solution. Similar as curve 2 in Figure 2, the two oxidation and two reduction reactions are indicated as I_a, II_a, II_c and III_c. The current of the oxidation process II_a and the current of the reduction reaction III_c grow with increasing scan number. This also seems to be the case for process I_a but this is due to the fact that the offset of the redox reaction is higher because of the increase of reaction II_a. Running several times through the potential window is needed to observe all redox processes. This can be explained by the fact that the gelatin matrix should be repressed by the buffer solution before getting the optimal redox reactions.
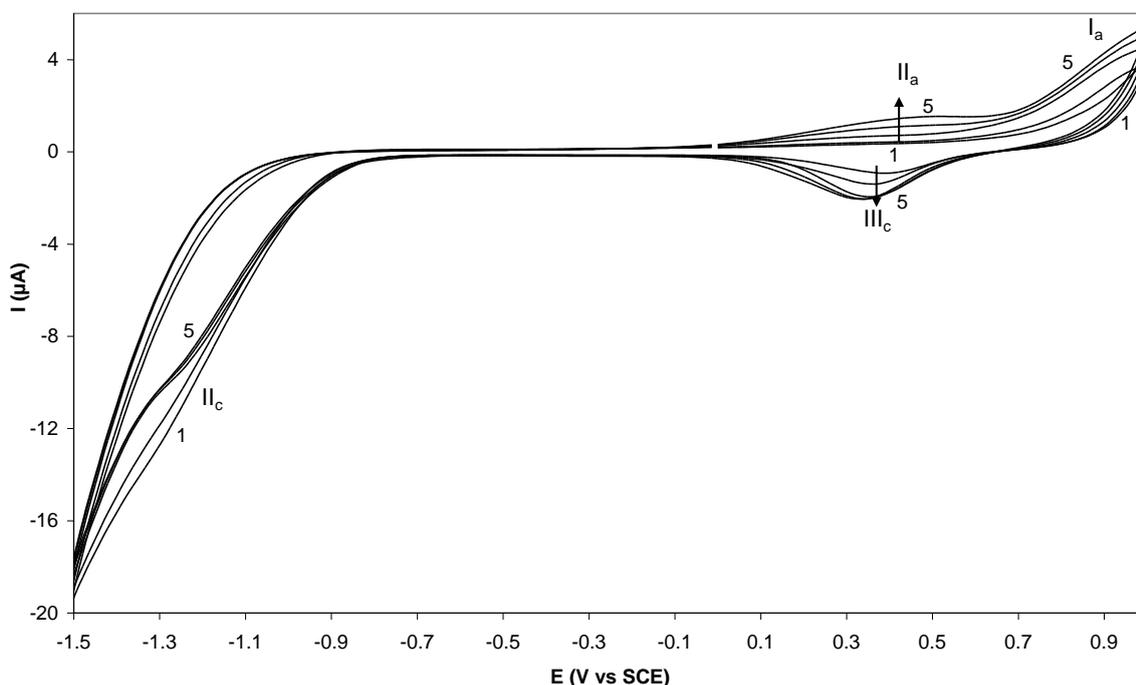

Figure 6. The current potential behaviour of a GelB|Au electrode in a 10 mmol.L^{-1} HEPES pH 7 buffer solution as a function of scan number: scan 2 (1), 3 (2), 10 (3), 15 (4) and 20 (5).

3.3. Comparison of the electrochemical behavior of a gold electrode modified with GelA and GelB

Figure 7 represents the cyclic voltammetric behaviour of a GelA|Au (dashed line) and a GelB|Au (full line) electrode in a 10 mmol.L^{-1} HEPES pH 7 buffer solution in a potential window from -1.5 versus 1 V with a scan rate of 50 mV.s^{-1}. A similar electrochemical behaviour is observed except for a potential shift of ca. 100 mV which is observed for the gelatin related reduction reaction (III_c).

This can be explained by the difference in charge of the gelatin immobilized onto the gold surface. The iso-electric point of GelB has a value of ca. 5, which results in a negative charge of GelB at physiological pH. GelA has a positive charge, as its iso-electric point is ca. 8, and is thus more easily reduced at the electrode, resulting in a more positive value for the reduction process of gelatin A. Nevertheless, both gelatin types can be used for encapsulation of biological components such as redox enzymes. Based on the nature and charge of the redox enzyme, the selection of a specific type of gelatin can be made.
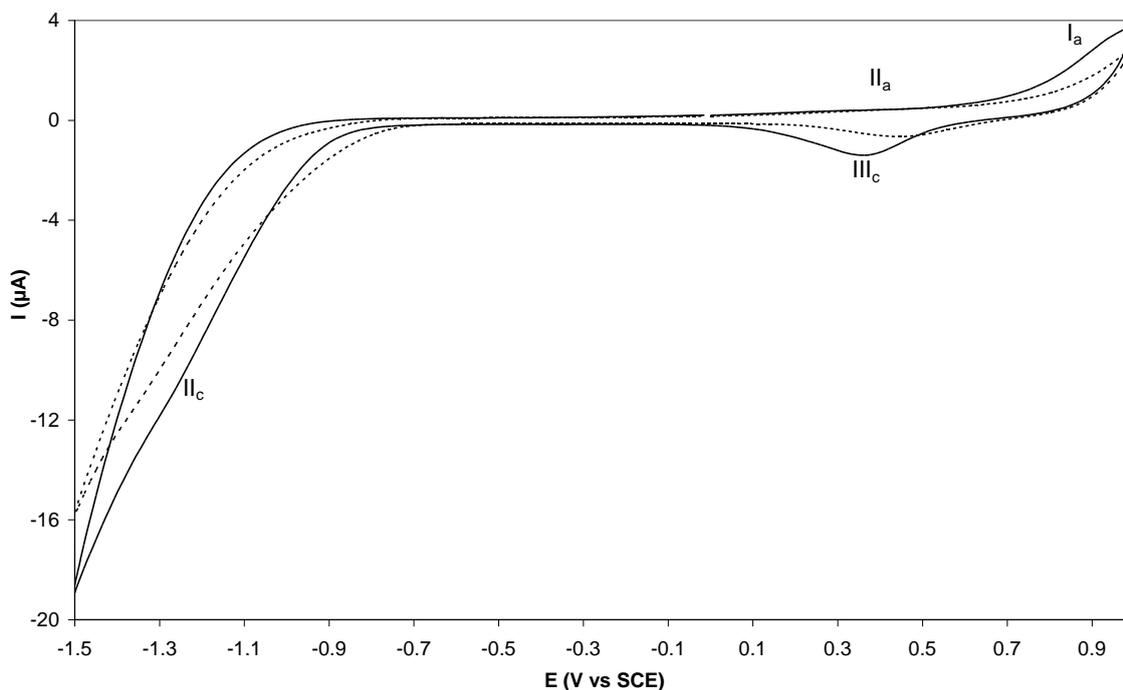

Figure 7. The current potential behaviour of a GelA|Au (dashed line) and a GelB|Au electrode (full line) in a 10 mmol.L^{-1} HEPES pH 7 buffer solution with a scan rate of 50 mV.s^{-1} in a potential window from −1.5 till 1 V.

4. CONCLUSIONS

The deposition of gelatin onto a gold electrode has been described in this article. ATR-IR spectroscopy proved to be a suitable tool to demonstrate the presence of gelatin on the gold electrode surface. The electrochemical behaviour of gelatin modified gold electrodes was studied in the potential window −1.5 till 1.0 V vs SCE by performing cyclic voltammetry. Redox processes due to the gold surface, the used HEPES buffer solution and the gelatin layer were identified. To avoid these interfering redox reactions, applying a reduced potential window is necessary to study the electrochemical behaviour of components that will be immobilized in the gelatin matrix. As a consequence, the useful potential window (i.e. no electrochemical background) is from −0.4 till 0.2 V vs SCE.

References

1. S.H. Nezhadi, P.F.M. Choong, F. Lotfipour and C.R. Dass, *J. Drug Targeting,* 17 (2009) 731
2. K.B. Djagny, Z. Wang and S. Xu, *Crit. Rev. Food Sci. Nutr.,* 41 (2001) 481
3. S.B. Lee, H.W. Jeon, Y.W. Lee, Y.M. Lee, K.W. Song, M.H. Park, Y.S. Nam and H.C. Ahn, *Biomaterials,* 24 (2003) 2503
4. J.E. Eastoe and A.A. Leach, Chemical constitution of gelatin, in: A.G. Ward, A. Courts (Eds.), *The science and technology of gelatin*, Academic Press, New York (1977)
5. L.H. Lin and K.M. Chen, *Colloids Surf.*, A 272 (2006) 8
6. P. Johns and A. Courts, Relationship between collagen and gelatin, in: A.G. Ward, A. Courts (Eds.), *The Science and Technology of Gelatin*, Academic Press, New York (1977)
7. W.E. Hennink and C.F. van Nostrum, *Adv. Drug Delivery Rev.,* 54 (2002) 13
8. E. Emregul, S. Sungur and U. Akbulut, *J. Biomater. Sci., Polym. Ed.,* 16 (2005) 505
9. S. Sungur and Y. Numanoglu, *Artif. Cells Blood Substit. Immobil. Biotechnol.,* 34 (2006) 41
10. S. Timur and U. Anik, *Anal. Chim. Acta,* 598 (2007) 143
11. M. Pohanka, D. Jun and K. Kuca, *Sensors,* 8 (2008) 5303
12. L. Zajoncova, M. Jilek, V. Beranova and P. Pec, *Biosens. Bioelectron,.* 20 (2004) 240
13. E. Logoglu, S. Sungur and Y. Yildiz, *J. Macromol. Sci., Part A: Pure Appl. Chem.,* 43 (2006) 525
14. J.H. Muyonga, C.G.B. Cole and K.G. Duodu, *Food Chem.,* 86 (2004) 325
15. K. De Wael, S. De Belder, S. Van Vlierberghe, G. Van Steenberge, P. Dubruel and A. Adriaens, *Talanta* 82 (2010) 1980
16. A. Barth, *Biochim. Biophys. Acta, Bioenerg.,* 1767 (2007) 1073
17. Y. Abe and S. Krimm, *Biopolymers,* 11 (1972) 1817
18. M. Jackson, L. Choo, P.H. Watson, W.C. Halliday and H.H. Mantsch, *Biochim. Biophys. Acta, Mol. Basis Dis.,* 1270 (1995) 1
19. B.E. Conway, *Prog. Surf. Sci.,* 49 (1995) 331
20. D.J. Trevor, C.E.D. Chidsey and D.N. Loiacono, *Phys. Rev. Lett.,* 62 (1989) 929
21. S.K. Trabelsi, N.B. Tahar, B. Trabelsi and R. Abdelhedi, *J. Appl. Electrochem.,* 35 (2005) 967